

Radiation from Flux Flow in Josephson Junction Structures

L. N. Bulaevskii¹ and A. E. Koshelev²

We derive the radiation power from a single Josephson junction (JJ) and from layered superconductors in the flux-flow regime. For JJ case, we formulate the boundary conditions for the electric and magnetic fields at the edges of the superconducting leads using the Maxwell equations in the dielectric media and find dynamic boundary conditions for the phase difference in JJ which account for the radiation. We derive the fraction of the power fed into JJ transformed into the radiation. In a finite-length JJ this fraction is determined by the dissipation inside JJ and it tends to unity as dissipation vanishes independently of mismatch of the junction and dielectric media impedances. We formulate also the dynamic boundary conditions for the phase difference in intrinsic JJs in highly anisotropic layered superconductors of the $\text{Bi}_2\text{Sr}_2\text{CaCu}_2\text{O}_8$ type at the boundary with free space. Using these boundary conditions, we solve equations for the phase difference in the linear regime of Josephson oscillations for rectangular and triangular lattices of Josephson vortices. In the case of rectangular lattice for crystals with the thickness along the c -axis much larger than the radiation wavelength, we estimate the radiation power per unit length in the direction of magnetic field at the frequency 1 THz as $\sim N \mu\text{W/cm}$ for $\text{Tl}_2\text{Ba}_2\text{CaCu}_2\text{O}_8$ and $\sim 0.04 N \mu\text{W/cm}$ for $\text{Bi}_2\text{Sr}_2\text{CaCu}_2\text{O}_8$. For crystals with thickness smaller than the radiation wavelength, we found that the radiation power in the resonance is independent on number of layers and can be estimated at 1 THz as 0.5 W/cm ($\text{Tl}_2\text{Ba}_2\text{CaCu}_2\text{O}_8$) and 24 mW/cm ($\text{Bi}_2\text{Sr}_2\text{CaCu}_2\text{O}_8$). For rectangular lattice, due to superradiation regime, up to half of power fed into the crystal may be converted into the radiation. In the case of triangular or random lattice in the direction perpendicular to the layers, the fraction of power converted into the radiation depends on the dissipation rate and is much lower than for rectangular lattice in the case of high-temperature superconductors with nodes in the gap.

1. INTRODUCTION

In 1962, Josephson [1] predicted electromagnetic radiation from superconducting tunneling junction arguing that in the presence of voltage V across the junction the phase difference φ changes with time as $\partial\varphi/\partial t = 2eV/h$, while the tunneling current density J changes as $J = J_c \sin(2eVt/h)$. Here J_c is the critical superconducting current via the junction. Thus, the photons with the Josephson frequency $\omega = 2eV/h$ may be emitted from Josephson junction (JJ). Such a

radiation from JJ into the waveguide with the power $\mathcal{P}_{\text{rad}} \sim 10^{-12}$ W has been detected by Dmitrenko *et al.* [2] and Langenberg *et al.* [3] soon after the Josephson prediction. The junction in both experiments was subject to bias current and dc magnetic field applied parallel to the junction. The dc magnetic field induces Josephson vortices, and they move to the JJ edge in the presence of the transport current across the junction, causing oscillations of the magnetic and electric fields inside JJ and in superconducting leads around JJ. More precisely, flux flow induces electromagnetic (Swihart) waves inside JJ, and they are partially transmitted outside when hit JJ edges [4]. From measurements of the current–voltage (I – V) characteristics, Langenberg *et al.* [3] found the power $\mathcal{P} = IV$ fed into the junction and the fraction

¹Los Alamos National Laboratory, Los Alamos, New Mexico 87545.

²Materials Science Division, Argonne National Laboratory, Argonne, Illinois 60439.

converted into radiation, $Q = \mathcal{P}_{\text{rad}}/\mathcal{P} \approx 10^{-5}$. Theoretically, Q was estimated as a ratio of the impedances of JJ modeled as a strip line and the waveguide [3,5]:

$$Q_Z = \frac{4Z_0Z_s}{(Z_0 + Z_s)^2} \sim \left(\frac{8\lambda d}{\varepsilon w^2} \right)^{1/2}, \quad (1)$$

where Z_0 is the waveguide impedance, Z_s is the strip line impedance in the limit $k_\omega w \ll 1$ and $Z_s \ll Z_0$. Here λ is the London penetration length of the superconducting leads, d is the thickness of the insulating layer, ε_i is its dielectric constant, $k_\omega = \omega/c$ and w is the junction width. Equation (1) gives $\approx 10^{-5}$ for the studied junction in agreement with experimental value. Thus, low radiation power from JJ was attributed to the mismatch between the impedances of the junction and the waveguide. To the best of our knowledge, no deeper theoretical treatment of radiation was made after that and the concept of the impedance mismatch for a single JJ and later for layered superconductors with intrinsic JJ was accepted by the community.

As radiation from the vortex flow in a single junction was found to be quite low, a natural idea was proposed to use multiple lock-in junctions. Then, in the super-radiation regime, radiation power may be enhanced by the factor N^2 , where N is the number of synchronized junctions inside the space of the radiation wavelength. Intensive theoretical and experimental study was done in this direction, see, e.g., [6–12]. However, an effective way to synchronize many junctions was not found so far. There are two problems to overcome for synchronization. The first one is the technologically inevitable variation of parameters from junction to junction, mainly J_c parameter, which affects operating frequency of the junction at given current. The second problem is that the coherent locked-in flow of the Josephson vortices in different junctions is unstable in a wide range of parameters.

The discovery of layered high-temperature superconductivity added new breath into this activity. It was recognized that the Bi- and Tl-based cuprate superconductors with weakly coupled superconducting CuO_2 layers exhibit the same static and dynamical Josephson properties as artificial tunneling junctions. In another words, the crystals $\text{Bi}_2\text{Sr}_2\text{CaCu}_2\text{O}_8$ (BSCCO) and $\text{Tl}_2\text{Ba}_2\text{CaCu}_2\text{O}_8$ (TBCCO) represent a stack of many intrinsic JJs on the atomic scale [13]. The first indication of the intrinsic Josephson effect was observation of switching of individual junc-

tions to the resistive state in the I - V characteristics [14]. After that, many Josephson effects have been found in these systems including the Fraunhofer patterns in the dependence of the critical current on the dc magnetic field applied parallel to the layers [15], Josephson plasma resonance [16] strongly affected by pancake vortices in the presence of the magnetic field applied perpendicular to the layers [17,18], Shapiro steps in the I - V characteristics induced by external microwave radiation [19,20], and Fiske resonances [21–23].

One can anticipate much smaller variations of intrinsic-junction parameters in comparison with the artificially-fabricated junction arrays. In addition, the intrinsic junctions are much closer to each other and one can anticipate much stronger coupling between them. What is more, there are many junctions on the scale of the radiation wavelength, and so they will super-radiate when synchronized. Due to these advantages, the moving Josephson vortex lattice in layered superconductors was proposed as a source of monochromatic tunable continuous electromagnetic radiation in the terahertz frequency range [24–27]. Experimentally, radiation from the high-temperature layered superconductor BSCCO at relatively low frequencies, 7–16 GHz, was detected by Hechtfisher *et al.* [28]. Some indirect evidence of radiation at higher frequencies has been recently reported by Kadowaki *et al.* [29] and Batov *et al.* [30] reported radiation at the frequency 0.5 THz with power 1 pW from BSCCO mesa consisting 100 junctions in zero dc magnetic field.

Therefore, it is interesting to estimate theoretically the possible radiation power generated by a moving vortex lattice and find optimal conditions for generation. For that we need to understand the mechanism of conversion of the electromagnetic field associated with the flux flow of the Josephson vortices into the electromagnetic waves outside of the JJ and find limitations imposed by this mechanism in Josephson structures. A natural first step is to understand at the microscopic level the conversion mechanism in a single JJ. Then such an approach may be extended to layered structures.

In the first part, we consider radiation from a single JJ. Then, the method to treat radiation is extended to intrinsic junctions in layered superconductors. We will show that super-radiation regime is inherent to moving rectangular vortex lattice in such crystals. We will discuss the consequences of this regime for the radiation power and I - V characteristics.

Radiation From Flux Flow in Josephson Junction Structures

1.1. Radiation from a Single Josephson Junction

As we discussed in Section 1, a common way to evaluate the radiation out of a single JJ is to take product of the total power supplied to the junction, $\mathcal{P} = IV$ and the impedance mismatch coefficient Q_Z , Eq. (1). A weak point of this impedance approach for real, finite-length JJ is ignoring of multiple reflections inside the junction, i.e., assumption that the propagating electromagnetic wave has only one attempt to escape the JJ, decaying before reflected wave reaches another edge. In fact, at low dissipation rate (low temperature and low dielectric losses inside the insulating layer) reflections lead to the formation of almost standing Swihart waves inside JJ. In this case, Q strongly depends on the dissipation and approaches unity as dissipation vanishes. Then the question turns out to be what are limitations on \mathcal{P} and \mathcal{P}_{rad} rather than on Q .

However, the standard analysis of *transport properties* of finite-size JJs uses sine-Gordon equation and zero-derivative boundary conditions for the oscillating part of the phase at the edges [5,31–33]. At the JJ edges vanishing oscillating magnetic field $B = \partial\varphi/\partial x$ leads to zero Poynting vector. Thus, for such boundary conditions, the outside radiation is absent and all supplied power dissipates inside JJ.

In the following, we reconsider this problem, discuss the power conversion mechanism and derive the radiation power from a single JJ into free space in the case when w is much larger than the wavelength of outgoing electromagnetic wave. This is not realistic limit, but it is a simplest one which demonstrates the method to treat radiation and which may be directly extended to the case of smaller w . Our rigorous approach is based on solution of the Maxwell equations inside the superconducting leads and in outside space, which allowed us to formulate accurate dynamic boundary conditions for the oscillating phase inside JJ. In the linear regime of Josephson oscillations, we obtained analytical results for \mathcal{P}_{rad} and Q using the perturbation theory. In this regime, we found that $Q \propto Q_Z \mathcal{N}$, where \mathcal{N} is the number of reflections before Swihart wave decays inside JJ. At low temperatures in JJ made out of gapped superconductors with perfect insulating layer, \mathcal{N} may be large compensating small Q_Z . Our approach also opens the way for numerical calculations in general case, when linear approach is invalid.

The JJs with low level of the dissipation become available now due to the perspective to use them as a qubits for quantum computing [34]. The radiation

should be stronger in such junctions in comparison with previously studied ones. This gives additional motivation to reconsider the theoretical background of the radiation from JJ.

To find outside radiation due to the Josephson oscillations, one has to match oscillating fields inside the junction and in the superconducting leads with the wave solution outside the junction. Expressing the oscillating fields inside the junctions via the phase difference, we derive dynamic boundary conditions for the phase difference and relate the Poynting vector of radiation to the phase difference at junction edge. The final step is the solution of the equations for the phase difference accounting for the dynamic boundary conditions and derivation of the Poynting vector.

1.2. Equation for the Phase Difference

We consider a JJ with the length $l \gg \lambda$ located at $-l < x < 0$ and bounded by dielectric with dielectric constant ϵ_d , see Fig. 1. Strength of the coupling in the junction is characterized by the Josephson current density J_c and related parameters: the Josephson length, $\lambda_J = \sqrt{c\Phi_0/(8\pi^2\Lambda J_c)}$, and plasma frequency, $\omega_p = \sqrt{8\pi^2 d c J_c / (\epsilon_i \Phi_0)}$, where $\Lambda = 2\lambda + d$. We consider the simplest situation when the JJ width along z direction, w , is larger than both λ_J and wavelength of outgoing electromagnetic wave. We will consider straight Josephson vortices along the external magnetic field. In this approach the problem becomes one dimensional for the phase difference and two dimensional for the electric and magnetic fields in the outer space as both of them become z -independent. We consider junction in resistive state and assume that the junction phase, $\bar{\varphi}$, oscillates with the

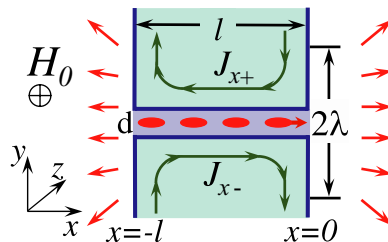


Fig. 1. A finite-size JJ opened into free space at both edges. Ellipses illustrate the moving vortex lattice. Curved lines show the screening currents inside the superconducting leads, arrows show radiation from area 2λ around the junction. The applied dc magnetic field H_0 is along the z -axis.

Josephson frequency ω generating oscillating electric (E_x and E_y) and magnetic (B_z) fields inside the junction and in the superconducting leads. Our task is to find spatial distribution of these fields and match them with outside fields to find equation and boundary conditions for $\bar{\varphi}$.

We first derive equation for the oscillating magnetic field inside the superconducting leads. We use complex representation for the oscillating fields and phase, e.g.,

$$\bar{\varphi}(x, t) = \langle \bar{\varphi}(x, t) \rangle_t + \sum_{\omega} \text{Re}[\bar{\varphi}_{\omega}(x)e^{-i\omega t}].$$

Here, $\langle \dots \rangle_t$ means time average. The phase gradient is connected by the following relation with the magnetic field inside the junction and supercurrents flowing along the junction at the opposite sides

$$\nabla_x \bar{\varphi} = \frac{8\pi^2 \lambda^2}{c\Phi_0} [J_{x+} - J_{x-}] - \frac{2\pi d}{\Phi_0} B_z. \quad (2)$$

From Maxwell equations, material equation for current inside superconductor, $\mathbf{J} = (c/4\pi\lambda^2)[(\Phi_0/2\pi)\nabla\phi - \mathbf{A}] + \sigma_q \mathbf{E}$, London relation for the electric field, $\mathbf{E} = -(4\pi\lambda^2 i\omega/c)\mathbf{J}$, and Eq. (2), we derive the following equation for the oscillating magnetic field inside the leads ($-\ell < x < 0$) at $d \ll \lambda$

$$(\nabla_x^2 + \nabla_y^2)B_z(\omega) - \frac{B_z(\omega)}{\lambda_{\omega}^2} = \frac{\Phi_0}{2\pi\lambda^2} \frac{\partial \bar{\varphi}_{\omega}}{\partial x} \delta(y), \quad (3)$$

$$\lambda_{\omega}^{-2} = \lambda^{-2} - \varepsilon_s k_{\omega}^2 + 4\pi i k_{\omega} \sigma_q / c, \quad k_{\omega} = \omega/c. \quad (4)$$

We ignore small contribution to the magnetic field from the dc current flowing via the junction. The ac electric field inside the superconducting leads is $E_y(\omega, x, y) = i\lambda_{\omega}^2 k_{\omega} \nabla_x B_z(\omega, x, y)$. To obtain the total electric field in the junction area, one has to account also for the field inside the dielectric layer. This gives

$$E_y(\omega, x, y) = -\frac{i\omega\Phi_0}{2\pi c} \bar{\varphi}_{\omega}(x)\delta(y) + i\lambda_{\omega}^2 k_{\omega} \nabla_x B_z(\omega, x, y). \quad (5)$$

The boundary condition for $\bar{\varphi}_{\omega}(x)$ follows from the boundary condition for the electric field

$$-i\omega[\varepsilon_d E_x(+0, y) - \varepsilon E_x(-0, y)] = 4\pi J_x(-0, y).$$

As $E_x(-0, y) = -i\omega(4\pi\lambda^2/c^2)J_x(-0, y)$, we obtain

$$4\pi(1 - \varepsilon k_0^2 \lambda^2)J_x(-0, y) = -i\omega\varepsilon_d E_x(+0, y). \quad (6)$$

As the electric field $E_x(+0, y)$ is continuous at $y = 0$, this means that $J_x(0, y)$ also must be continuous and from Eq. (2) in the limit $d \ll \lambda$ we obtain

$$\nabla_x \bar{\varphi}_{\omega}(0) = \nabla_x \bar{\varphi}_{\omega}(-l) = 0. \quad (7)$$

We can represent solution of Eq. (3) near the edge $x = 0$ as

$$\begin{aligned} B_z(x, y) &= B_b(x, y) - \frac{\Phi_0}{(2\pi\lambda)^2} \int_{-\infty}^0 \nabla_{x'} \bar{\varphi}_{\omega}(x') dx' \\ &\times [K_0(c_-) - K_0(c_+)], \\ c_{\pm} &= \sqrt{(x \pm x')^2 + y^2/\lambda_{\omega}}, \end{aligned} \quad (8)$$

where $K_0(z)$ is the modified Bessel function and $B_b(x, y)$ is the solution of the homogeneous equation

$$(\nabla_x^2 + \nabla_y^2)B_b - \lambda_{\omega}^{-2}B_b = 0, \quad (9)$$

with the boundary condition $B_b(-0, y) = B_z(+0, y)$. As a function of x , $B_b(x, y)$ decays at distance $\sim \lambda$ from the boundary. For its Fourier transform along the y -direction, we obtain $[k_x = (\lambda_{\omega}^{-2} + k_y^2)^{1/2}]$

$$B_b(\omega, x, y) = \int \frac{dk_y}{2\pi} B_z(+0, k_y) \exp(-\kappa_x |x|).$$

For static case, distribution of the magnetic field near the edge of JJ has been recently derived by A. Gurevich (unpublished).

Using Maxwell equation $\nabla_x B = (i\omega\varepsilon_i/c)E_y - (4\pi/c)J_y$, Josephson relation $E_y(x, 0) = -i\omega\Phi_0\bar{\varphi}_{\omega}(x)/(2\pi cd)$, and Eq. (8), we find equation for the oscillating phase

$$\begin{aligned} \left(\frac{\omega^2}{\omega_p^2} + \alpha_t \frac{i\omega}{\omega_p}\right) \bar{\varphi}_{\omega}(x) + \frac{\lambda_J^2}{\pi\lambda} \int_{-\infty}^0 dx' \nabla_x \left[K_0\left(\frac{x-x'}{\lambda_{\omega}}\right) \right. \\ \left. + K_0\left(\frac{x+x'}{\lambda_{\omega}}\right) \right] \nabla_{x'} \bar{\varphi}_{\omega}(x') - \frac{c\nabla_x B_b(x, 0)}{4\pi J_c} = s_{\omega}(x), \end{aligned} \quad (10)$$

where $s_{\omega}(x)$ is the complex amplitude of the oscillating Josephson current, $\sin[\bar{\varphi}(x, t)] = \text{Re}[s_{\omega}(x) \exp(-i\omega t)]$, and $\alpha_t = \omega_p \sigma_t \Phi_0 / (2\pi J_c cd)$ is damping due to the tunneling quasiparticle conductivity. In static case, similar nonlocal equation has been derived by Gurevich [35]. In the case $\lambda \ll \lambda_J$ and $|x| \gg \lambda$, non-locality is not essential, and Eq. (10) can be reduced to usual local approximate equation

$$\left(\frac{\omega^2}{\omega_p^2} + \alpha_t \frac{i\omega}{\omega_p}\right) \varphi_{\omega} + \lambda_J^2 \left(1 - \alpha_q \frac{i\omega}{\omega_p}\right) \nabla_x^2 \varphi_{\omega} = s_{\omega}(x), \quad (11)$$

where $\alpha_q = 2\pi\lambda^2\omega_p\sigma_q/c^2$ is the dissipation due to quasiparticles inside superconductor and we used expansion $\lambda_{\omega}/\lambda \approx 1 - 2\pi i\lambda^2 k_{\omega}\sigma_q/c$ neglecting k_{ω}^2 term.

Radiation From Flux Flow in Josephson Junction Structures

1.3. Boundary Conditions and the Poynting Vector

Near the boundary situation is more complicated because, in addition to smoothly changing part, the phase has component decaying at distances of order λ from the boundary. This extra phase is smaller than the smooth phase by the factor $\sim \lambda/\lambda_J$ but it has comparable derivative. Our purpose is to derive accurate boundary condition for the smooth phase, $\varphi_\omega(x)$, obeying Eq. (11). For this we integrate Eq. (10) from intermediate distance $-x_i$ with $\lambda \ll x_i \ll \lambda_J$ up to the boundary $x = 0$. Neglecting small terms proportional to x_i and $B_b(-x_i, 0)$ [for $B_z(0, y) \ll \Phi_0/(4\pi\lambda^2)$], using local approximation at $x = -x_i$, we obtain the boundary condition for the smooth phase in a very simple form

$$\nabla_x \varphi_\omega(0) \approx \nabla_x \bar{\varphi}_\omega(-x_i) = -\frac{\lambda}{\lambda_\omega} \frac{4\pi\lambda}{\Phi_0} B_z(\omega, \mathbf{r} = 0). \quad (12)$$

This equation can be compared with condition (7) for *the total phase*. Equation (12) allows us reduce the problem to solution of local Eq. (11) for smooth phase with modified boundary conditions and avoid solving exact integral equation for the total phase, Eqs. (7) and (10).

For that we need to express $B_z(\mathbf{r} = 0)$ via φ_ω . Relation between the electric and magnetic field at the boundary is determined by properties of outside media.

1.4. Outside Dielectric Media

We consider first outside dielectric media with dielectric constant ε_d . In the situation $\omega k_\omega \gg 1$, in the straight-vortices approach, outside fields are z -independent. In addition, if we assume that the dielectric media is infinite in y direction and the thickness of the leads is much larger than λ , we can use Fourier transform in this direction. In this case, the Fourier components of fields with $|k_y| < \sqrt{\varepsilon_d} k_\omega$ propagate in the media, while the field components decay with $|k_y| > \sqrt{\varepsilon_d} k_\omega$. In particular, for $E_y(\omega, x, k_y)$ we have

$$E_y(\omega, x, k_y) = \begin{cases} E_y(\omega, 0, k_y) \exp[i\sqrt{\varepsilon_d k_\omega^2 - k_y^2} \text{sign}(\omega)x], \\ \text{for } |k_y| < \sqrt{\varepsilon_d} k_\omega, \\ E_y(\omega, 0, k_y) \exp[-\sqrt{k_y^2 - \varepsilon_d k_\omega^2} x], \\ \text{for } |k_y| > \sqrt{\varepsilon_d} k_\omega. \end{cases} \quad (13)$$

Other field components, E_x and B_z , can be expressed via $E_y(\omega, 0, k_y)$. First, $E_x(\omega, x, k_y)$ can be obtained from Eq. (13) and Maxwell equation $\nabla \mathbf{E} = 0$ and then $B_z(\omega, x, k_y)$ can be obtained using the Maxwell equation $(\Delta \times \mathbf{E})_z = ik_\omega B_z$ which gives

$$B_z(\omega, x, k_y) = \frac{\varepsilon_d |k_\omega|}{\sqrt{\varepsilon_d k_\omega^2 - k_y^2}} E_y(\omega, 0, k_y) \times \exp[i\sqrt{\varepsilon_d k_\omega^2 - k_y^2} \text{sign}(\omega)x], \quad \text{for } |k_y| < \sqrt{\varepsilon_d} k_\omega, \\ B_z(\omega, x, k_y) = \frac{-i\varepsilon_d k_\omega}{\sqrt{k_y^2 - \varepsilon_d k_\omega^2}} E_y(\omega, 0, k_y) \times \exp\left[-\sqrt{k_y^2 - \varepsilon_d k_\omega^2} x\right], \quad \text{for } |k_y| > \sqrt{\varepsilon_d} k_\omega, \quad (14)$$

In particular, this gives relation between fields at the boundary, which we will use to formulate the boundary conditions for the phase

$$B_z(0, k_y) = \zeta(\omega, k_y) E_y(0, k_y), \\ \zeta(\omega, k_y) = \begin{cases} |k_\omega| \varepsilon_d / \sqrt{\varepsilon_d k_\omega^2 - k_y^2}, & \text{for } |k_y| < \sqrt{\varepsilon_d} k_\omega, \\ -ik_\omega \varepsilon_d / \sqrt{k_y^2 - \varepsilon_d k_\omega^2}, & \text{for } |k_y| > \sqrt{\varepsilon_d} k_\omega. \end{cases} \quad (15)$$

Note again that the term $\zeta(\omega, k_y)$ for $|k_y| < \sqrt{\varepsilon_d} k_\omega$ originates from outgoing electromagnetic wave (radiation), while the term $\zeta(\omega, k_y)$ for $|k_y| > \sqrt{\varepsilon_d} k_\omega$ is due to the wave decaying at distance $\sim (k_y^2 - \varepsilon_d k_\omega^2)^{-1/2}$ from the lead boundaries. The latter term does not carry energy out of the junction. For completeness, we also present this important relation in the frequency-space representation

$$B_z(\omega, 0, y) = \int dy' U(\omega, y - y') E_y(\omega, 0, y'), \\ U(\omega, y) = \frac{\varepsilon_d}{2} [|k_\omega| J_0(\sqrt{\varepsilon_d} k_\omega y) + ik_\omega N_0(\sqrt{\varepsilon_d} k_\omega y)]. \quad (16)$$

where $J_0(z)$ and $N_0(z)$ are the Bessel functions, and in the time-space representation

$$B_z(t, 0, y) = \sqrt{\varepsilon_d} \frac{\partial}{\partial t} \int dt' dy' \frac{\Theta[c_d^2(t-t')^2 - (y-y')^2]}{\sqrt{c_d^2(t-t')^2 - (y-y')^2}} \times E_y(t', 0, y') \quad (17)$$

where $\Theta(x) = 1$ if $x > 0$ and 0 if $x < 0$ and $c_d = c/\sqrt{\varepsilon_d}$.

Now we will relate boundary fields with the phase. From Eqs. (5) and (8) follows the relation

$$E_y(0, k_y) = i\lambda_\omega^2 k_\omega \kappa_x B_z(0, k_y) - \frac{ik_\omega \Phi_0}{2\pi} \left(\varphi_\omega(0) - \frac{\lambda_\omega^2}{\lambda^2} \int_{-\infty}^0 \exp(\kappa_x x) \nabla_x \varphi_\omega(x) dx \right). \quad (18)$$

This relation and Eq. (15) allow us to express the boundary fields via the phase distribution

$$E_y(0, k_y) = \frac{B_z(0, k_y)}{\zeta(\omega, k_y)}, \quad B_z(0, k_y) = \frac{\Phi_0}{2\pi} \frac{i\zeta k_\omega}{1 - i\zeta\lambda_\omega^2 k_\omega \kappa_x} \times \left(-\varphi_\omega(0) + \frac{\lambda_\omega^2}{\lambda^2} \int_{-\infty}^0 \exp(\kappa_x x) \nabla_x \varphi_\omega(x) dx \right) \quad (19)$$

Typically, $\zeta\lambda_\omega^2 k_\omega \kappa_x \sim \lambda\omega/c \ll 1$. Also $\Delta_x \varphi_\omega(x) \sim \varphi_\omega(x)/\lambda_J$ and the integral term in Eq. (19) is smaller than $\varphi_\omega(0)$ by the parameter λ/λ_J . Therefore, we obtain

$$E_y(0, k_y) \approx \frac{\Phi_0}{2\pi} ik_\omega \varphi_\omega(0), \quad B_z(0, k_y) \approx \frac{\Phi_0}{2\pi} i\zeta k_\omega \varphi_\omega(0). \quad (20)$$

Within this approximation, the magnetic field at the junction edge which determines the boundary condition (12) is

$$B_z(\mathbf{r} = 0) \approx -\frac{\Phi_0}{2\pi} ik_\omega \varphi_\omega(0) Z(\omega), \quad Z(\omega) \approx \int_{-\pi/d}^{\pi/d} \frac{dk_y}{2\pi} \zeta(\omega, k_y) \approx \frac{\varepsilon_d |k_\omega|}{2} - i \frac{\varepsilon_d k_\omega}{\pi} \ln \frac{\pi/d}{\sqrt{\varepsilon_d} |k_\omega|}. \quad (21)$$

Finally, we obtain the boundary conditions for smooth oscillating phase at both edges, $x = 0, -l$, in a finite-length JJ:

$$\nabla_x \varphi_\omega(x) \approx \pm 2i\lambda k_\omega Z(\omega) \varphi_\omega(x), \quad \text{for } x = 0, -l. \quad (22)$$

Radiation outside JJ to the right is given by the Poynting vector, $\mathcal{P}_{\text{rad}} = (c/4\pi) \int dy \langle E_y(0, y, t) B_z(0, y, t) \rangle_t$,

$$\mathcal{P}_{\text{rad}} \approx \frac{\varepsilon_d W \omega^3 \Phi_0^2}{64\pi^3 c^2} |\varphi_\omega(0)|^2. \quad (23)$$

We also present the phase equation and boundary conditions in the time representation. Introducing the dimensionless variables $\tau = \omega_p t$, and $u = x/\lambda_J$

and using Eq. (11), we write the equation for the total smooth phase $\varphi(\tau, u)$, which includes both oscillating and non-oscillating components

$$\left[\frac{\partial^2}{\partial \tau^2} - \nabla_u^2 + (\alpha_t - \alpha_q \nabla_u^2) \frac{\partial}{\partial \tau} \right] \varphi + \sin \varphi = 0. \quad (24)$$

Using Eqs. (12), (21), and (22) and adding the boundary condition for the static phase, we obtain the dynamic boundary condition:

$$\nabla_u \varphi(\tau, 0) = -b - \int_{-\infty}^{\tau} d\tau' \mathcal{K}(\tau - \tau') \frac{\partial \varphi(\tau', 0)}{\partial \tau'}, \quad \mathcal{K}(\tau) = \frac{d\varepsilon_d}{2\pi \varepsilon_i \lambda_J} \frac{\partial}{\partial \tau} \left[\frac{\mathcal{F}(\xi \tau)}{\tau} \right], \quad \mathcal{F}(v) = \int_0^v dz J_0(z). \quad (25)$$

Here, $\xi = \pi c/(\omega_p d \sqrt{\varepsilon_d})$, $J_0(z)$ is the Bessel function, $b = 4\pi\lambda\lambda_J H_0/\Phi_0$ with $\mathbf{H}_0 \parallel z$ being the applied dc magnetic field, $b \ll \lambda_J/\lambda$. For the edge $x = -l$ we need to change sign of \mathcal{K} . Due to the non-analytical ω -dependence of $Z(\omega)$, the kernel $\mathcal{K}(\tau)$ is irregular at $d \rightarrow 0$ and then $\tau \rightarrow 0$. Singular frequency dependence of $Z(\omega)$ is due to retardation caused by electromagnetic wave propagation inside dielectric, Eq. (17). Thus, boundary conditions also exhibit retardation effect.

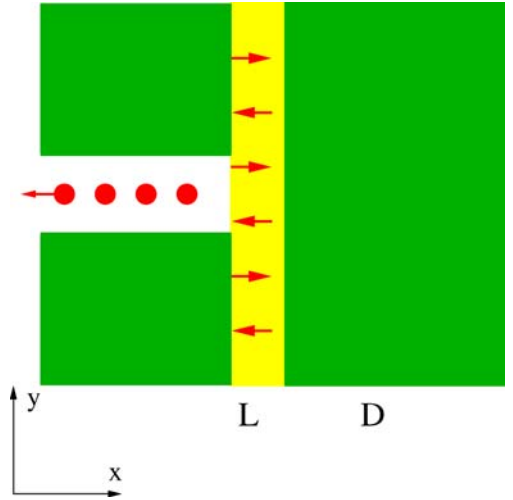


Fig. 2. The JJs at $x < 0$, dielectric at $0 < x < L \ll k_\omega^{-1}$ and superconducting screen with the London penetration length λ_s and the thickness $D \gg \lambda_s$. Such a screen effectively reflects the Swihart wave back into the junction. It introduces additional interaction of vortices in different junctions in the case of multiple parallel junctions.

2. OUTSIDE SUPERCONDUCTING SCREEN

Let us consider now a junction with superconducting screen at the right side separated from the layered crystal by the dielectric with the thickness L small in comparison with the wave length of the electromagnetic wave in this dielectric, see Fig. 2. Such a screen prevents the radiation from the right side increasing it from other side. In the case of many parallel junctions, the screen enhances their interaction as was suggested by Ivanchenko [11].

At $k_\omega L \ll 1$ we can neglect effect of the dielectric on the boundary conditions as fields in the dielectric are the same as at the edge of the superconducting screen. Fields inside the superconducting screen obey Eq. (9). The solution is

$$\begin{aligned} E_y(\omega, x, y) &= \frac{1}{(2\pi)^2} \int_{-\infty}^{+\infty} dk_y G(k_y) e^{-\kappa_x x + ik_y y}, \\ \kappa_x &= \sqrt{\lambda_{s,\omega}^{-2} + k_y^2}, \\ E_x(\omega, x, y) &= -\frac{1}{(2\pi)^2} \int_{-\infty}^{+\infty} dk_y G(k_y) \frac{k_y}{\kappa_x} e^{-\kappa_x x + ik_y y}, \\ B_z(\omega, x, y) &= -\frac{1}{(2\pi)^2} \int_{-\infty}^{+\infty} dk_y G(k_y) \frac{\lambda_{s,\omega}^{-2}}{ik_\omega \kappa_x} e^{-\kappa_x x + ik_y y}, \end{aligned} \quad (26)$$

where $\lambda_{s,\omega}$, given by Eq. (4), characterizes the superconducting screen and λ_s is the London penetration length of the screen. From this solution, we obtain

$$\begin{aligned} B_z(\omega, \mathbf{r} = 0) &= -\frac{\Phi_0}{2\pi} ik_\omega \varphi_\omega(0) Z_s(\omega), \quad (27) \\ Z_s(\omega) &= \frac{i}{\pi k_\omega \lambda_{s,\omega}^2} \ln \left(\frac{1}{\lambda_s d} \right) \end{aligned}$$

This leads to the boundary condition

$$\frac{\partial \varphi_\omega(0)}{\partial u} = \eta \varphi_\omega(0), \quad \eta \approx \frac{2\lambda_J \lambda}{\pi \lambda_s^2} \ln \left(\frac{1}{\lambda_s d} \right) \quad (28)$$

Note that $\eta \gg 1$. This results in the condition that $\varphi_\omega(0)$ is very close to zero for screened edge of the junction, while at the open edge the condition is that space derivative is close to zero. There is flow of energy from closed edge proportional to the small parameter $4\pi\lambda_s^2\sigma_q/c$ due to quasiparticle dissipation inside the screen.

3. SOLUTION FOR THE PHASE DIFFERENCE, I - V CHARACTERISTICS, RADIATION, AND DISSIPATION POWER

Now we solve analytically Eq. (24) using the perturbation theory with respect to the Josephson current [31,32] in the limit $|b - \tilde{\omega}|/b \gg 1$. Taking solution as

$$\varphi(\tau, u) = \tilde{\omega}\tau - bu + \theta(\tau, u), \quad \theta(\tau, u) \ll 1, \quad (29)$$

and expanding $\sin[\varphi(\tau, u)]$, we see that $\theta_\omega(u) \equiv \theta(\tilde{\omega}, u)$ obeys reduced versions of Eq. (11) with $s_\omega = -e^{ibu}/i$,

$$[\nabla_u^2 + \tilde{\omega}^2 + i\tilde{\omega}(\alpha_t - \alpha_s \Delta_u^2)]\theta_\omega(u) = -e^{ibu}/i. \quad (30)$$

and boundary conditions (22)

$$\frac{d\varphi}{du} = \pm i\tilde{\omega}\beta\varphi, \quad \text{for } u = 0, -\tilde{l} \quad (31)$$

with

$$\beta = \beta_0 \left(|\tilde{\omega}| - \frac{2i\tilde{\omega}}{\pi} \ln \frac{\pi c/d}{\sqrt{\varepsilon_d \omega_p} |\tilde{\omega}|} \right), \quad \beta_0 = \frac{\varepsilon_d d}{2\varepsilon_i \lambda_J}$$

Solution for $\theta(\tilde{\omega}, u)$ given by,

$$\theta_\omega(u) \approx -\frac{e^{ibu}/i}{\tilde{\omega}^2 - b^2 + i\alpha_b \tilde{\omega}} + a_1 e^{ip_\omega u} + a_2 e^{-ip_\omega u}, \quad (32)$$

describes the moving vortex lattice (the first term) and reflected Swihart waves propagating to the right and left. Here $\alpha_b = \alpha_t + \alpha_q b^2$ and $p_\omega = \sqrt{(\tilde{\omega}^2 + i\alpha_q \tilde{\omega})/(1 - i\alpha_q \tilde{\omega})} \approx \tilde{\omega} + i\alpha/2$ with $\alpha = \alpha_t + \alpha_q \tilde{\omega}^2$. For a JJ with both open edges finding a_1 and a_2 from the boundary conditions (31) we obtain the phase distribution

$$\begin{aligned} \theta_\omega(u) &= -\frac{\exp(ibu)/i}{\tilde{\omega}^2 - b^2 + i\alpha_b \tilde{\omega}} \\ &\quad - \{(b - \beta\tilde{\omega}) [\cos[p_\omega(\tilde{l} + u)] - i\tilde{\beta} \sin[p_\omega(\tilde{l} + u)]] \\ &\quad - (b + \beta\tilde{\omega}) \exp(-ib\tilde{l}) [\cos(p_\omega u) + i\tilde{\beta} \sin(p_\omega u)]\} / \\ &\quad \{(\tilde{\omega}^2 - b^2 + i\alpha_b \tilde{\omega}) p_\omega [(1 + \tilde{\beta}^2) \sin(p_\omega \tilde{l}) \\ &\quad + 2i\tilde{\beta} \cos(p_\omega \tilde{l})]\} \end{aligned}$$

with $\tilde{\beta} \equiv \beta\tilde{\omega}/p_\omega$ and $\tilde{l} = l/\lambda_J$. Alternatively, the phase was obtained by expansion with respect to eigenmodes [31, 32]. In particular, the boundary values which determine outside irradiation are given by

$$\begin{aligned} \theta_\omega(0) &= \frac{i}{\tilde{\omega}^2 - b^2 + i\alpha_b \tilde{\omega}} \\ &\quad \times \left[1 - \frac{(b - \beta\tilde{\omega}) [\cos(p_\omega \tilde{l}) - i\tilde{\beta} \sin(p_\omega \tilde{l})] - (b + \beta\tilde{\omega}) \exp(-ib\tilde{l})}{ip_\omega [(1 + \tilde{\beta}^2) \sin(p_\omega \tilde{l}) + 2i\tilde{\beta} \cos(p_\omega \tilde{l})]} \right] \end{aligned}$$

$$\theta_\omega(-\tilde{l}) = \frac{i \exp(-i b \tilde{l})}{\tilde{\omega}^2 - b^2 + i \alpha_b \tilde{\omega}} \times \left[1 - \frac{(b - \beta \tilde{\omega}) \exp(i b \tilde{l}) - (b + \beta \tilde{\omega}) [\cos(p_\omega \tilde{l}) - i \beta \sin(p_\omega \tilde{l})]}{i p_\omega [(1 + \beta^2) \sin(p_\omega \tilde{l}) + 2 i \beta \cos(p_\omega \tilde{l})]} \right]$$

These cumbersome formulae can be significantly simplified in the regime $b \gg \tilde{\omega}$, weak dissipation $\alpha_t, \alpha_q \ll 1$, and large impedance mismatch, $|\beta| \ll 1$. In this case, keeping only Fiske resonance terms, we obtain

$$\begin{aligned} \theta_\omega(0) &\approx [\cos(p_\omega \tilde{l}) - \exp(-i b \tilde{l})]/(\tilde{\omega} b D), \\ \theta_\omega(-1) &\approx [1 - \exp(-i b \tilde{l}) \cos(p_\omega \tilde{l})]/(\tilde{\omega} b D), \\ D &\approx \sin(\tilde{\omega} \tilde{l}) + i(2\beta + \alpha \tilde{l} 2) \cos(\tilde{\omega} \tilde{l}), \end{aligned} \quad (33)$$

In these approximate results, we also neglected the term $\text{Im} [\beta(\omega)]$, which only slightly shifts resonance positions. Radiation to the right and left, $\mathcal{P}_{\text{rad}}^{r,l}(\tilde{\omega}, b)$, is determined by the values $|\theta_\omega(0)|^2$ and $|\theta_\omega(-1)|^2$. At low dissipation, $\alpha \tilde{l} \ll 1$, we derive

$$\begin{aligned} \mathcal{P}_{\text{rad}}^{r,l} &\approx \frac{\Phi_0^2 \omega \omega_p^2 \omega}{64 \pi^3 c^2 b^2} \frac{1 - 2 \cos(b \tilde{l}) \cos(\tilde{\omega} \tilde{l}) + \cos^2(\tilde{\omega} \tilde{l}) \pm \rho}{|D|^2}, \\ \rho &= 2(\alpha \tilde{l} + 2\beta)[1 - \cos(b \tilde{l}) \cos(\tilde{\omega} \tilde{l})] b. \end{aligned} \quad (34)$$

The radiation reaches maxima for almost standing Swihart waves at frequencies $\tilde{\omega} = \tilde{\omega}_n = \pi n / \tilde{l}$ with $n = 1, 2, \dots$, when $\cos(b \tilde{l}) \cos(\tilde{\omega}_n \tilde{l}) \neq 1$. The resonance width is determined by both, the dissipation, $\alpha \tilde{l}$, and by the radiation, β . The perturbation theory is valid in resonance for $|\theta_\omega(0)| \sim (b \alpha \tilde{l} \tilde{\omega})^{-1} < 1$ and the radiation power in this linear regime is quite small, $\mathcal{P}_{\text{rad}}/\omega \lesssim 10^{-6}$ and $\lesssim 1 \mu\text{W}/\text{cm}$ at $\nu = 10 \text{ GHz}$ and 1 THz , respectively. The asymmetry of radiation described by ρ is small.

Next we derive the dc current at voltage $V = \Phi_{0\omega}/(2\pi c)$ and estimate Q . The current I via JJ is given by the tunneling quasiparticle contribution, $I_t = \sigma_t V l \omega / d$, and the Josephson current contribution, I_s ,

$$I_s(\omega) \approx J_c l \omega i_j \quad (35)$$

$$i_j = \tilde{l}^{-1} \int_{-\tilde{l}}^0 du \langle \cos(\tilde{\omega} \tau - bu) \theta(\tau, u) \rangle_\tau. \quad (36)$$

The exact result for the reduced Josephson current, i_j , is given by

$$\begin{aligned} i_j &= \frac{\alpha_b \tilde{\omega} / 2}{(\tilde{\omega}^2 - b^2)^2 + \alpha_b^2 \tilde{\omega}^2} \\ &+ \text{Im} \left[\frac{(b^2 + \beta^2 p_\omega^2) [\cos(b \tilde{l}) - \cos(p_\omega \tilde{l})] + i \beta [(b^2 + p_\omega^2) \sin(p_\omega \tilde{l}) - 2 p_\omega b \sin(b \tilde{l})]}{i p_\omega (p_\omega^2 - b^2) (\tilde{\omega}^2 - b^2 + i \alpha_b \tilde{\omega}) [(1 + \beta^2) \sin(p_\omega \tilde{l}) + 2 i \beta \cos(p_\omega \tilde{l})]} \right] \end{aligned} \quad (37)$$

In the case of weak dissipation, the total Josephson current can be split into the dissipation and radiation parts, $I_s = I_{s,\text{dis}} + I_{s,\text{rad}}$. The radiation part plays the same role as dissipation because in both cases energy is transferred from the moving vortex lattice to other degrees of freedom (to photons in the case of radiation). In the lowest order in $\lambda/\lambda_J \ll 1$ at the resonance frequencies we get

$$I_{s,\text{dis}} \approx \frac{\alpha \varepsilon_i \omega_p l}{2 \varepsilon_d \omega d} I_{s,\text{rad}} \approx \frac{\Phi_0 c \omega \alpha \tilde{l} \sin^2(b \tilde{l} / 2)}{32 \pi^2 \lambda \lambda_j b^2 \tilde{\omega} |D|^2}. \quad (38)$$

Losses due to radiation are equivalent to those caused by a resistor with $R\omega = 2\pi/(\varepsilon_d \omega)$ attached parallel to JJ ($Rw \approx 90 \Omega \text{ cm}$ for $\varepsilon_d = 1$ and $\nu = 10 \text{ GHz}$). The power fed into JJ is $\mathcal{P} = IV$. Part of it, $(I_t + I_{s,\text{dis}})V$, is dissipated inside JJ, while another part, $I_{s,\text{rad}}V$, is radiated. Neglecting non-resonant part, I_t , we obtain for the radiated fraction, $Q \equiv \mathcal{P}_{\text{rad}}/\mathcal{P}$,

$$Q = \text{Re}[\beta] \frac{\tilde{\omega}}{2 \tilde{l}} \frac{|\theta_\omega(0)|^2 + |\theta_\omega(-1)|^2}{\alpha_i \tilde{\omega} + i_j}. \quad (39)$$

In the regime of weak dissipation and near resonances we approximately obtain

$$Q \approx \frac{r}{1+r}, \quad r = \frac{I_{s,\text{rad}}}{I_{s,\text{dis}}} = \frac{2 \varepsilon_d d \omega}{\varepsilon_i \omega_p \alpha \tilde{l}}. \quad (40)$$

To clarify the physical meaning of the parameter r , we can represent it as $r = Qz(\omega \gg k_\omega^{-1})\mathcal{N}$ where

$$Qz(\omega \gg k_\omega^{-1}) = \frac{2 \varepsilon_d d \omega}{\varepsilon_i \lambda_J \omega_p} \ll 1$$

is the transmission coefficient of the electromagnetic wave at the junction edge (impedance mismatch) into free space in the limit $wk_\omega \ll 1$ and $\mathcal{N} = 1/\alpha \tilde{l}$ is the number of reflections before the Swihart wave decays inside JJ. At $wk_\omega \sim 1$ and our result is larger than that given by Eq. (1) by the factor \mathcal{N} . As dissipation inside JJ decreases (σ_t and σ_q drop), \mathcal{N} increases. As one can see from Eq. (40), the relation between the dissipative and radiative dampings is mainly determined by competition between the two small parameters, α and d/l . In the linear regime, $b \alpha \tilde{l} \tilde{\omega} > 1$, we get $\mathcal{N} < b \tilde{\omega}$. Due to limitation $b < \lambda_J/\lambda$ we obtain $Q \lesssim (d/\lambda) \tilde{\omega}^2 \sim 10^{-2} (\omega/\omega_p)^2$.

Figure 3 shows three-dimensional plots illustrating dependencies of the total reduced current density $J/J_0 = \alpha_t \tilde{\omega} + i_j$ and the radiated fraction Q on the Josephson frequency ω (voltage) and field b . For illustration purposes we used toy parameters, $\tilde{l} = 4$, $\alpha_t = 0.01$, $\alpha_q = 0$, and $\beta_0 = 0.001$. Figure 4 shows

Radiation From Flux Flow in Josephson Junction Structures

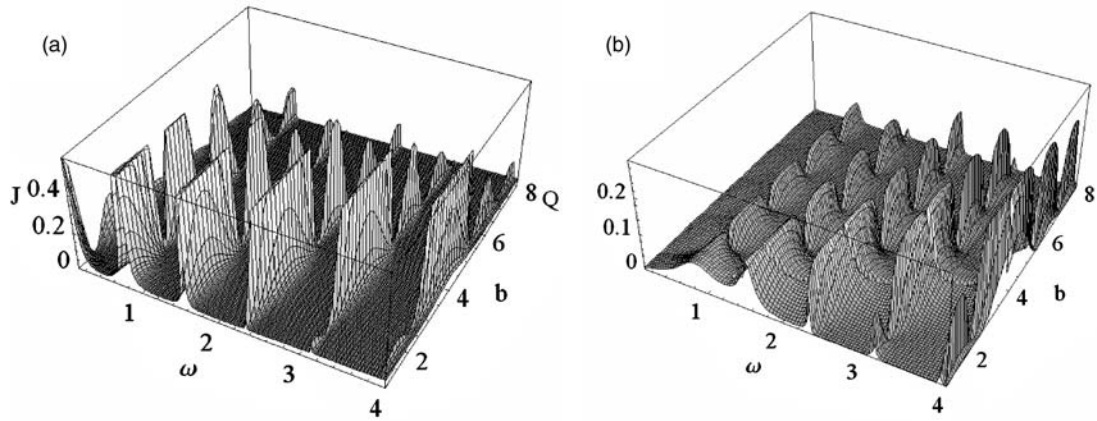


Fig. 3. Three-dimensional plots of the current density (left plot) and the radiated fraction (right plot) for $\bar{l} = 4$, $\alpha_t = 0.01$, $\alpha_q = 0$, and $\beta_0 = 0.001$ obtained within linear approximation.

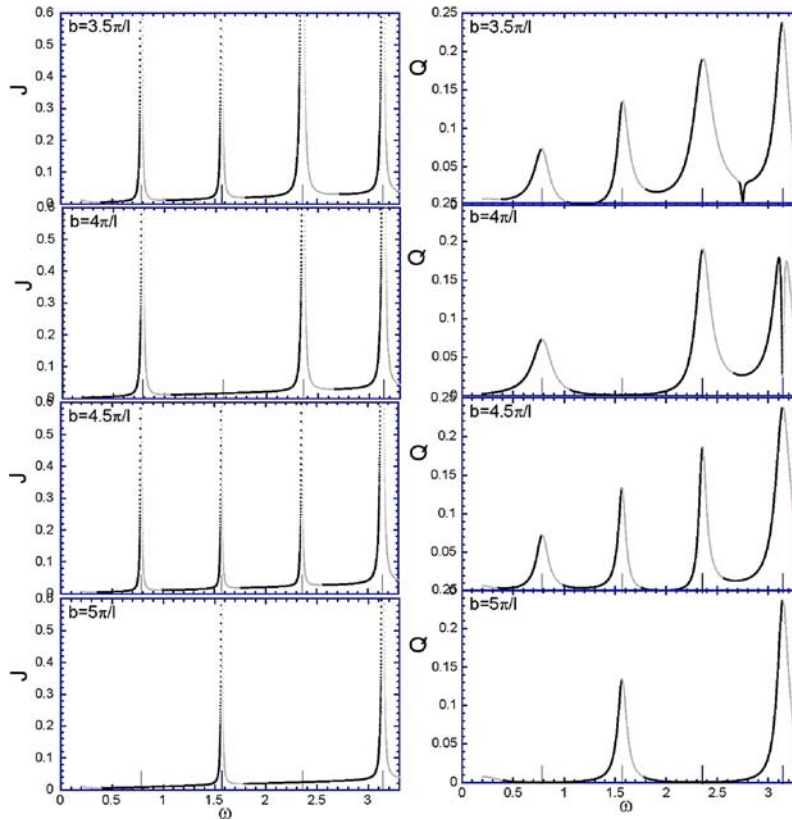


Fig. 4. The voltage dependencies of J and Q at several fields for the same parameters as in the previous plot. The current shows sharp increases near the marked Fiske-resonance frequencies. The linear approximation does not describe narrow regions near the resonances. Q reaches maxima given by Eq. (40) at the resonances. In the plots for $b = 3.5\pi/l \approx 2.75$ and $4\pi/l \approx 3.53$ one can see sharp drops of Q at the frequencies, corresponding to the Eck resonance condition $\tilde{\omega} = b$.

voltage dependencies of J and Q for several fields. The current shows well-known sharp peaks at the Fiske-resonance frequencies, and peak amplitudes oscillate with the magnetic field [31–33]. The conversion coefficient Q shows smooth oscillating behavior reaching maxima given by estimate (40) at the resonances. We also observe another nontrivial feature, Q sharply drops at the position corresponding to the Eck resonance conditions, $\tilde{\omega} = b$, even though no feature is seen in I – V dependencies for this frequency. For comparison, we also plotted in Fig. 5 the same dependencies for the case of higher dissipation, $\alpha_t = 0.1$. This case is quantitatively described by the linear approximation and allows us to trace switching between different Fiske peaks with increasing current.

For a JJ with closed and open edges we obtain

$$\begin{aligned} \theta_\omega(0) &\approx -\sin(p\omega\tilde{l})/(\tilde{\omega}bD), \\ D &\approx \cos(\tilde{\omega}\tilde{l}) + (i/2)(\beta + \alpha\tilde{l})\sin(\tilde{\omega}\tilde{l}), \end{aligned} \quad (41)$$

The Poynting vector of radiation from open edge at $x = 0$ is given by the expression

$$\mathcal{P}_{\text{rad}} \approx \frac{\Phi_0^2 \omega \omega_p^2 \omega \sin^2(\tilde{\omega}\tilde{l})}{64\pi^3 c^2 b^2 |D|^2}, \quad (42)$$

The I – V characteristics defined by Eq. (35) consists of maxima at the frequencies ω_n . The part of it, where $dI/dV < 0$, is unstable in the current-biased regime. Experimentally, only voltages corresponding to the resonance frequencies ω_n were observed [2,3]. Numerical calculations [6,7] show that such a behavior occurs in the nonlinear regime, i.e., at very low dissipation.

3.1. Conclusions for Single-Junction Case

We have shown that in the case of weakly dissipative junctions Q may become of order unity in the linear regime. Nevertheless, the radiation power per unit width, $\mathcal{P}_{\text{rad}}/w$, given by Eq. (23), is always small in this regime because *the condition* $|\theta_\omega| \lesssim 1$ *also restricts the power fed into JJ*. The open question is whether it is possible to get $|\theta_\omega| \gg 1$ and larger \mathcal{P}_{rad} in strongly nonlinear regime when dissipation is very low and many Swihart modes are involved. The I – V characteristics in this limit have the form of sharp steps (Fiske steps) according to experimental data [2,3] and numerical calculations [6,7]. However, the amplitude $\varphi_\omega(0)$, which determines the radiation

power, in highly nonlinear regime was not calculated yet.

In conclusion, accounting for the radiation into the dielectric outside media, we derived the dynamic boundary conditions for JJ with the width ω much larger than the wave length of the electromagnetic wave radiated into the free space. The method of derivation may be extended to the case $wk_\omega \ll 1$ and following qualitative conclusions are valid for this case as well. We have shown that in the linear regime of Josephson oscillations the radiated fraction Q of the power fed into the junction is determined by the number of multiple reflections (i.e., by dissipation rate inside JJ) and by the transmission coefficient, Q_Z , from JJ into free space. Even if Q reaches unity, radiation power per unit width of JJ remains small in the linear regime. To probe radiation power from JJ in the nonlinear regime, numerical study based on Eqs. (24) and (25) is needed. We think that measurements of radiation in the best junctions available now, like those studied in [34], at low temperatures and at intermediate magnetic fields may show higher radiation than that observed previously.

4. RADIATION IN LAYERED SUPERCONDUCTORS

For layered superconductors we need to formulate equations for the phase differences $\varphi_n(t, x)$ inside each intrinsic junction n between layers n and $n + 1$ as well as the boundary conditions for these variables. Here coordinates of layers are $y = (n + 1/2)s$ and layers are parallel to the plane (x, z) . In general φ_n depend also on the coordinate z , the direction of the applied magnetic field H_0 , but we will neglect this dependence (straight-vortex approach) assuming that width of the crystal along the z -axis is much larger than the radiation wavelength, $k_\omega w \gg 1$. The derivation of equations for $\varphi_n(t, x)$ [36–38] is similar to that for a single JJ. Using the Maxwell equations, the expression for the intralayer supercurrents via the phase of the superconducting order parameter inside layers and the Josephson relation for interlayer current one need to exclude all variables describing intralayer currents and electromagnetic fields induced by these currents by expressing them via φ_n . Formulation of the boundary conditions is also similar to a single-junction case and is based on Eq. (16). However, solution of the equations for phase differences is now much more complicated because

Radiation From Flux Flow in Josephson Junction Structures

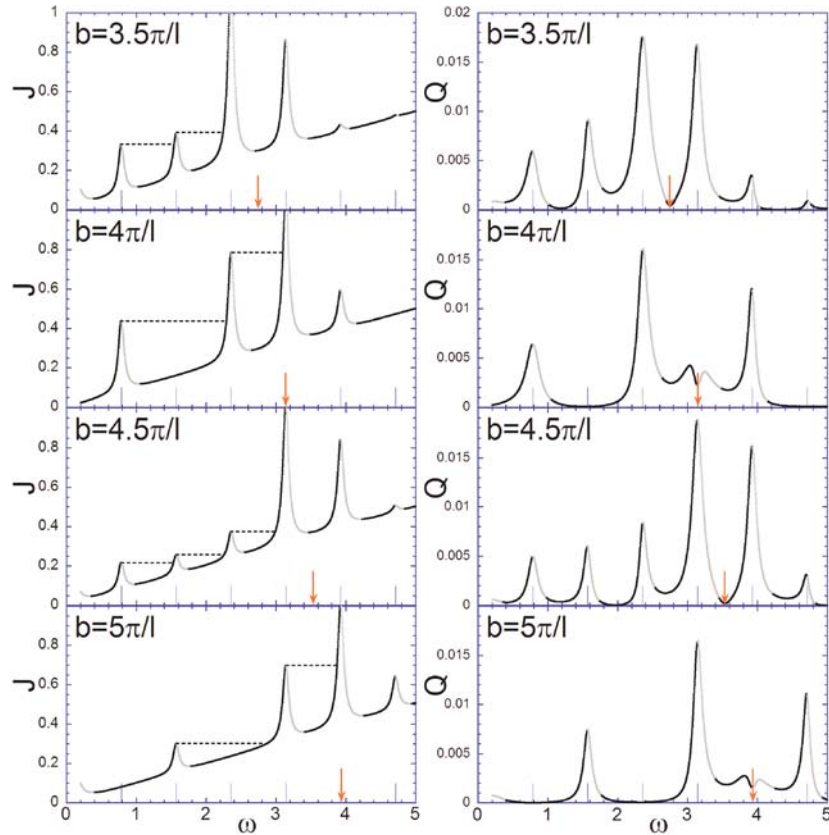


Fig. 5. The voltage dependencies of current J and radiated fraction, Q , at several fields for the higher dissipation $\alpha_l = 0.1$ (other parameters are the same as in the previous plots). Both J and Q show maxima near the marked resonance frequencies. Arrow marks frequency corresponding to the Eck resonance condition $\omega = b$. With current sweep the system will switch between different peaks, as it is illustrated by the dashed lines.

the vortex structure is two-dimensional (along x - and y -axes) and may vary depending on the parameters such as the applied dc magnetic field H_0 , the length l along the x -axis and also on the transport current (velocity of moving lattice). To have significant radiation power motion of vortex lattice in different intrinsic junction should be synchronized, as in multiple artificial JJ. For that interaction of intrinsic junctions should be strong enough and it should favor in-phase vortices in all junctions, i.e rectangular vortex lattice. First, we present the equations and the boundary conditions for $\varphi_n(t, x)$ and then discuss solutions for these equations and corresponding radiation power in linear regime of Josephson oscillations when perturbation theory may be used to solve equations for the phase differences. We will focus on crystals with large number of layers on the scale of the London penetration length λ_{ab} for intralayer currents. In this case, super-radiation from many layers becomes possible when there are many junctions on

the scale of radiation wavelength and when vortices in many junctions are synchronized. We will show that in this case significant part of the energy fed into the crystal is converted into the radiation.

4.1. Equations for the Phase Differences

The crystal length l is along the x -axis, while the transport current is perpendicular to the layers. Thus, the Josephson vortex lattice moves along the x -axis, see Fig. 6.

As we assumed that there is no dependence of the phase difference, current density \mathbf{j} , and the electromagnetic fields on z -coordinate, the components j_z , E_z , B_x , and B_y vanish. The phase difference $\varphi_n(t, x)$ between the layers n and $n + 1$ is defined as

$$\varphi_n(t, x) = \Phi_n - \Phi_{n+1} - \frac{2\pi}{\Phi_0} \int_{n_s}^{(n+1)_s} dy A_y(x), \quad (43)$$

where Φ_n is the phase of the superconducting order parameter inside the layer. Intrinsic junction n is in the space $(n - 1/2)s < y < (n + 1/2)s$. If N intrinsic JJs are identical then the dynamics of the system can be described by reduced coupled equations for the phase differences, $\varphi_n(t, x)$, and reduced magnetic fields $h_n = B_y(y = ns)/B_c$ with $B_c \equiv \Phi_0/(2\pi\lambda_{ab}\lambda_c)$ (see. e.g., [40])

$$\frac{\partial^2 \varphi_n}{\partial \tau^2} + v_c \frac{\partial \varphi_n}{\partial \tau} + \sin \varphi_n - \frac{\partial h_n}{\partial u} = 0, \quad (44)$$

$$\left(\nabla_n^2 - \ell^{-2} \left(1 + v_{ab} \frac{\partial}{\partial \tau} \right) \right) h_n + \left(1 + v_{ab} \frac{\partial}{\partial \tau} \right) \frac{\partial \varphi_n}{\partial u} = 0. \quad (45)$$

Here we used reduced x coordinate, $u = x/\lambda_J$ normalized to the Josephson length $\lambda_J = \gamma s$ and reduced time, $\tau = \omega_p t$, where $\omega_p = c/(\lambda_c \sqrt{\epsilon_c})$ is the plasma frequency, ϵ_c is the c -axis high-frequency dielectric constant inside the superconductor, λ_{ab} and λ_c are the London penetration lengths, $\ell \equiv \lambda_{ab}/s$, s is the interlayer distance, and ∇_n^2 notates the discrete second derivative operator, $\nabla_n^2 A_n = A_{n+1} + A_{n-1} - 2A_n$. The dissipation parameters, $v_{ab} = 4\pi\sigma_{ab}/(\gamma^2\epsilon_c\omega_p)$ and $v_c = 4\pi\sigma_c/(\epsilon_c\omega_p)$, are determined to the quasiparticle conductivities, σ_{ab} and σ_c , along and perpendicular to the layers, respectively. The conductivity σ_{ab} plays the same role as the conductivity σ_q for a single JJ. Applying the operator $\nabla_n^2 - \ell^{-2}(1 + v_{ab}\frac{\partial}{\partial \tau})$ to the first equation and excluding h_n , we can also de-

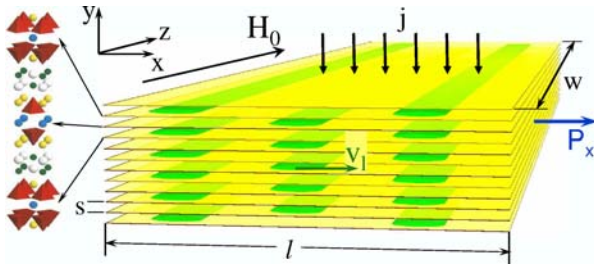


Fig. 6. Schematic picture of layered structure of superconductor and Josephson vortex lattice. The unit cell of $\text{Bi}_2\text{Sr}_2\text{CaCu}_2\text{O}_8$ compound and the relation of the crystal structure to the layered model are shown in the left. The directions of the applied dc magnetic field H_0 , of the dc transport current j , and of the radiation Poynting vector P_x are also shown. The Josephson vortices forming a triangular lattice are shown schematically by elliptical cylinders and v_1 is the velocity of moving lattice.

rive equations containing only $\varphi_n(u, \tau)$

$$\left[\nabla_n^2 - \ell^{-2} \left(1 + v_{ab} \frac{\partial}{\partial \tau} \right) \right] \left(\hat{T}_c \frac{\partial \varphi_n}{\partial \tau} + \sin \varphi_n \right) + \left(1 + v_{ab} \frac{\partial}{\partial \tau} \right) \frac{\partial^2 \varphi_n}{\partial u^2} = 0, \quad (46)$$

with $\hat{T}_c \equiv \partial/\partial \tau v_c$. Equation (46) represent just charge conservation laws. The first term describes the change of electron charges inside the layers and Cooper-pair interlayer tunneling currents, while the second term describes superconducting intralayer currents. The terms with the coefficient v_{ab} describe quasiparticle dissipative in-plane currents induced by moving Josephson vortices. The static interaction of junctions is described by the term $\nabla_n^2 \sin \varphi_n$, while their dynamic interaction is described by the term $T_c(\partial/\partial \tau)\nabla_n^2 \varphi$. Both are short-range (nearest-neighbor) weak interactions and they are not very effective in keeping long-range ordering of vortex lattice along the y -axis.

In the system of finite number of layers N the dc current with the density J is injected in layer 1 and extracted from layer N . Then equations for the first and the last junction are obtained from Eq. (46) by putting $\varphi_0 = \varphi_{N+1} = 0$ in linear terms and replacing $\sin \varphi_0 = \sin \varphi_{N+1} = j$. In a finite-layer system the edge junctions differ strongly from other junctions because they have only one neighboring junction.

The electric field inside the superconductor between layers n and $n + 1$ in terms of the phase difference is given as

$$E_{y;n,n+1} \approx \frac{\Phi_0}{2\pi s c} \frac{\partial \varphi_n}{\partial t}. \quad (47)$$

The average (over time or space) electric field determines the Josephson frequency ω_J . The average magnetic field we denote by B and we introduce dimensionless average magnetic field $b = 2\pi s \lambda_J B/\Phi_0$.

The parameters of BSCCO at low temperatures are $\omega_p/(2\pi) = 0.15$ THz, the Josephson critical current $J_c = 1700$ A/cm², $\gamma = 500$, $\epsilon_c = 12$, $s = 15.6$ Å, $\sigma_c(0) = 2 \times 10^{-3}$ (Ω cm)⁻¹, $\sigma_{ab}(0) = 4 \times 10^4$ (Ω cm)⁻¹ [44], and so $\ell \approx 100$, $v_{ab} \approx 0.2$ and $v_c \approx 5 \times 10^{-4}$. An important feature of the high-temperature superconductors is higher relative in-plane dissipation in comparison with c -axis dissipation, $v_{ab} \gg v_c$. Another layered high- T_c compound $\text{Tl}_2\text{Ba}_2\text{CaCu}_2\text{O}_8$ has lower anisotropy $\gamma \approx 150$ and as a consequence higher critical current $J_c \approx 3 \times 10^4$ A/cm² and higher plasma frequency, $\omega_p/(2\pi) \approx 0.75$ THz [45].

Radiation From Flux Flow in Josephson Junction Structures

4.2. Boundary Conditions and the Poynting Vector of Radiation

We assume that there are only outgoing waves and use Eq. (16) for an open edge. In the junction n , we approximate $B_z(y) \approx B_z(y_n)$ and $E_y(y) \approx E_y(y_n)$, where $y_n = sn$. This gives the following boundary condition at the boundary $x = 0$,

$$B_z(\omega, n) = \sum_m U(\omega, n-m) E_y(\omega, m), \quad (48)$$

$$U(\omega, n) \approx (1/2)s[|k_\omega|J_c(k_\omega sn) + ik_\omega N_0(k_\omega sn)], \quad n \neq 0,$$

while for $n=0$ we need to substitute $-(2/\pi) \ln [1/(|k_\omega|s)]$ for $N_0(k_\omega sn)$. Finally, we use the relations

$$B_z(t, n) = B_c \ell^2 \left[\frac{\partial \varphi_n}{\partial u} \right]_{x=0}, \quad E_y(t, n) = \frac{B_c \ell}{\sqrt{\epsilon_c}} \left[\frac{\partial \varphi_n}{\partial \tau} \right]_{x=0}, \quad (49)$$

to formulate the boundary condition for oscillating part of $\varphi_n(x, t)$. This gives the following general boundary conditions for the phase differences

$$\frac{\partial \varphi_n}{\partial u} = \pm \frac{is\omega}{2\ell\sqrt{\epsilon_c}} \sum_m [|k_\omega|J_0(k_\omega s|n-m|) + ik_\omega N_0(k_\omega s|n-m|)] \varphi_m \quad (50)$$

In the time representation we obtain again Eq. (17), as for a single junction.

For the Poynting vector, we derive

$$P_x(\omega) = \frac{\Phi_0^2 \omega^3}{64\pi^3 c^2 N_s} \times \sum_{n,m} J_0(k_\omega s|n-m|) \varphi_n(\omega, 0) \varphi_m^*(\omega, 0). \quad (51)$$

Let us consider now the layered superconductor with a superconducting screen at the right side separated from the layered crystal by the dielectric with thickness L small in comparison with the wavelength of the electromagnetic wave in this dielectric, see Fig. 7.

Then, as in the case of a single JJ, we neglect effect of the dielectric on the boundary condition. The solution inside the superconducting screen is given by Eq. (26). From this solution we obtain

$$B_z(\omega, y) = \frac{i\lambda_{s,\omega}^{-2}}{k_\omega} \int dy' N_0 \left(\frac{y-y'}{\lambda_{s,\omega}} \right) E_y(y'). \quad (52)$$

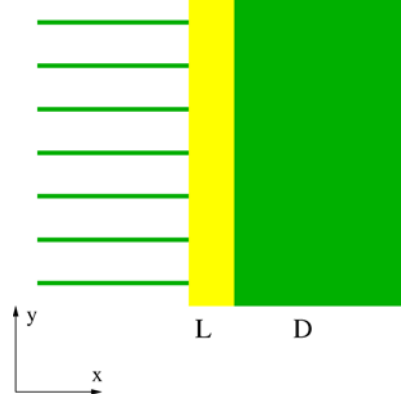


Fig. 7. The stack of intrinsic JJs at $x < 0$, dielectric at $0 < x < L \ll k_\omega^{-1}$ and a superconducting screen with the London penetration length λ_s and the thickness $D \gg \lambda_s$. Such a screen introduces additional interaction of vortices in different intrinsic junctions.

This relation leads to the boundary condition for the oscillating part of the phase difference

$$\frac{\partial \varphi_n(\omega, 0)}{\partial u} = \frac{\lambda_{Js}}{\lambda_{s,\omega}^2} \sum_m N_0 \left[\frac{s(n-m)}{\lambda_{s,\omega}} \right] \varphi_m(\omega, 0). \quad (53)$$

Here space derivative of the phase differences and the phase differences are at the point $x \rightarrow -0$. The space derivative now is not small, the parameter $(s\lambda_J/\lambda_s^2)$ may be of order unity or larger. The term in the free energy, \mathcal{F}_{bc} , corresponding to the boundary condition Eq. (53), is

$$\begin{aligned} \frac{\mathcal{F}_{bc}}{w} &= \int dy \int dx \frac{B_z^2}{4\pi} = \lambda_{s,\omega} s \sum_n \frac{B_z^2(sn)}{4\pi} \\ &= \frac{\Phi_0^2 s}{16\pi^3 \lambda_{s,\omega}^3} \sum_{n,m} H \left[\frac{s(n-m)}{\lambda_{s,\omega}} \right] \varphi_n(\omega, 0) \varphi_m^*(\omega, 0), \\ H(an) &= \sum_k N_0(ak) N_0[a(k+n)]. \end{aligned} \quad (54)$$

This free energy can be compared with the bulk inductive interaction, corresponding to Eq. (46), see [39],

$$\begin{aligned} \mathcal{F}_{ind} &= \frac{\Phi_0^2}{32\pi^3 \lambda_{ab} \lambda_c} \int du \nabla_u \varphi_n(u) \nabla_u \varphi_m(u) \\ &\times \exp \left[-\frac{|n-m|s}{\lambda_{ab}} \right]. \end{aligned} \quad (55)$$

Both interactions favor triangular lattice at least in the static case. The coefficient in Eq. (54) is much larger than that in the inductive free energy, i.e., superconducting screen enhances strongly the tendency

to form triangular lattice along the y -axis for not very large junction length l .

4.3. Solutions for the Phase Difference and the Radiation Power at High Fields in Large- N Case

We consider here the simplest case of layered crystals with large number of layers $N \gtrsim l$, when we can neglect edge effects along the y -axis, i.e., the difference between the edge (the first and the last) and inner junctions. This corresponds to the thickness larger than $0.2 \mu\text{m}$ with the total number of junctions $N > 100$.

In the linear regime of Josephson oscillations the general solution for the phase difference has the form

$$\varphi_n(\tau, u) = \tilde{\omega}\tau - bu + \kappa_n + \theta_n(\tau, u), \quad \theta_n(\tau, u) \ll 1. \quad (56)$$

For $\kappa_n = 0$ the lattice is rectangular, $\varphi_n = (\tau, u)$ are n -independent. For $\kappa_n = \pi n$ the lattice is triangular, vortices in neighboring layers are in anti-phase positions. For a static lattice such a configuration minimizes the energy of the magnetic field inside the crystal with large l, N . However, at small l boundary conditions are inconsistent with triangular lattice at some values of bl , and in this case rectangular lattice becomes more favorable [42]. For moving vortex lattice energy consideration does not work, and here the parameters k_n should be determined by the condition that total current I via each junction is the same [40],

$$J_c \lambda_J w \int_{-\bar{l}}^0 du \langle \sin \varphi_n(\tau, u) \rangle_\tau = I. \quad (57)$$

Slowly moving lattice preserves its triangular structure. This was confirmed experimentally via observation of magnetic oscillations of the flux-flow resistivity with the period of one flux quantum per two junctions [43]. Theoretical analysis [40,41] shows that the triangular lattice becomes unstable at the lattice velocity slightly smaller than the Swihart velocity $c_S = cs/(2\lambda_{ab}\sqrt{\epsilon})$. This instability corresponds to experimentally observed end point of the first flux-flow branch. It was also shown that interaction with top and bottom surfaces leads to significant lattice deformations [40].

Situation at high velocity $v_l \gg c_S$ is less clear. Lattice structures and their stability in this regime in the case of large lateral size ℓ have been addressed in [40] and have been reconsidered in [41] with the conclusion that for parameters typical for BSCCO no stable regular lattice exists at high velocities.

Structures and stability of steady states for small lateral sizes l is an open issue.

In the following sections we will estimate the radiation power for rectangular and triangular lattice and for lattice with random values of κ_n . Those are most probable realizations of vortex configurations in the large N limit. They give also an estimate for maximum radiation power which one can anticipate.

4.4. Rectangular Vortex Lattice

For rectangular lattice sketched at Fig. 8, $\varphi_n = \tilde{\omega}\tau - bu + \theta(\tau, u)$, the equation for the oscillating part, $\theta(u)$, is given by

$$\frac{\partial^2 \theta}{\partial \tau^2} + v_c \frac{\partial \theta}{\partial \tau} - \ell^2 \frac{\partial^2 \theta}{\partial u^2} \approx -\sin(\tilde{\omega}\tau - bu). \quad (58)$$

For a junction opened at both edges the solution is similar to that of a single JJ, Eq. (32). However, there is important difference due to the presence of large coefficient ℓ^2 in front of the second space derivative. This coefficient is due to uniformity of rectangular lattice and corresponding supercurrents along the y -axis, see Fig. 8. This uniformity leads to large energy of the magnetic field, i.e., inductive coupling, Eq. (55), *resulting in small amplitude of phase variations*. To find radiation power and I - V characteristics we use results of the perturbation theory for a single JJ. To make Eq. (58) similar to that for a single JJ we introduce $\tilde{u} = u/\ell$, $\tilde{b} = b\ell$, and \tilde{l} should be replaced by \tilde{l}/ℓ . We limit ourselves to the frequencies much smaller than the Eck

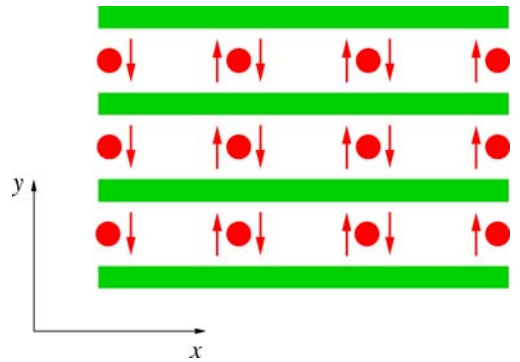


Fig. 8. Rectangular lattice of Josephson vortices in layered superconductors. The screening currents flow along the y -axis leading to the large energy of the magnetic field (inductive coupling). Correspondingly, the amplitude of phase modulation is weak, but vortices come to the junction edges coherently inducing super-radiation.

Radiation From Flux Flow in Josephson Junction Structures

resonance $\tilde{\omega} \ll b\ell$. In this case, the solution has the form $\theta(\tau, \tilde{u}) = \text{Re}[\theta_\omega \exp(-i\omega\tau)]$ with

$$\theta_\omega(u) \approx e^{i\tilde{u}}/(i\tilde{b}^2) + a_1 \exp(ip_\omega \tilde{u}) + a_2 \exp(-ip_\omega \tilde{u}), \quad (59)$$

The coefficients a_1 and a_2 should be found from the boundary conditions given by Eq. (50). For rectangular lattice at the edge $x = 0$ we obtain

$$\begin{aligned} \frac{\partial \theta_\omega(0)}{\partial \tilde{u}} &= \frac{i\tilde{\omega}}{2\sqrt{\epsilon_c}} s \\ &\times \sum_n [|k_\omega| J_0(k_\omega s n) + ik_\omega N_0(k_\omega s n)] \theta_\omega(0). \end{aligned} \quad (60)$$

Large number of junctions $N > (k_\omega s)^{-1}$

We consider first the case of very large number of layers $N > (k_\omega s)^{-1}$. Then

$$\frac{\partial \theta_\omega(0)}{\partial \tilde{u}} \approx \frac{i\tilde{\omega}}{\sqrt{\epsilon_c}} \theta_\omega(0). \quad (61)$$

This corresponds to $\beta \approx 1/\sqrt{\epsilon_c}$. Important point is that for such β the *perturbation theory is correct for $\tilde{\omega}|b\ell - \tilde{\omega}| \gg 1$, i.e., practically at all interesting fields and frequencies*. We limit ourself to the frequencies smaller than the Eck resonance $\tilde{\omega} \ll b$. Thus, the amplitude of Swihart waves is proportional to small factor ℓ^{-1} and oscillating part of the phase differences at $Nsk_\omega \gtrsim 1$ is described by Eq. (33) with the extra factor ℓ^{-1} for $\theta_\omega(0)$ and $\theta_\omega(-l)$. Further, we need to replace $\tilde{\omega}\tilde{l}$ by $\tilde{\omega}\tilde{l}/\ell \approx 0$, while in D we need to put $\beta = 1/\sqrt{\epsilon_c}$ and $\alpha = v_c$. Assuming that the length of junctions is small enough, $\tilde{\omega}\tilde{l} \ll \ell$ and using results Eq. (33) we see that oscillatory dependence of the radiation power and of the dc current on $\tilde{\omega}\tilde{l}$ drops out and we obtain for the dc current at $\tilde{\omega}b\ell \gg 1$ and $\tilde{\omega}\tilde{l} \ll \ell$ the expression *without resonances*

$$i = \frac{1}{J_c w \tilde{l}} = v_c \tilde{\omega} + \frac{\sqrt{\epsilon_c} |\sin(b\tilde{l}/2)|}{b^2 \ell \tilde{l}} \frac{1}{\tilde{\omega}}. \quad (62)$$

For the radiation power of N layers, using Eq. (51), we obtain

$$\frac{\mathcal{P}_{\text{rad}}}{w} \approx \frac{\Phi_0^2 \omega_p^2 \epsilon_c}{32\pi^3 c b^2 s \ell^2} N \sin^2(b\tilde{l}/2). \quad (63)$$

Comparing this result with that for a single junction, Eq. (34), we see that the additional factor $N/(k_\omega s \ell^2)$ is present. In BSCCO and TBCCO crystals at the frequency $\nu = 1$ THz the parameter $k_\omega s \ell^2 \sim 1$. Thus, the radiation power of N layers for a moving rectangular

lattice is $N/(k_\omega s)$ times larger than from a single intrinsic junction and additional large factor $1/(k_\omega s)$ is due to super-radiation in the case $Nk_\omega s \gtrsim 1$.

Let us discuss now the I - V characteristics given by Eq. (62). At a given current $i > i_{\text{min}}$ we have stable solution with positive slope, $dI/dV > 0$, at $\tilde{\omega} > \tilde{\omega}_{\text{min}}$. Here

$$\begin{aligned} \tilde{\omega}_{\text{min}} &= \left(\frac{\sqrt{\epsilon_c}}{b^2 \ell \tilde{l} v_c} \right)^{1/2} |\sin(b\tilde{l}/2)|, \\ i_{\text{min}} &= 2v_c \omega_{\text{min}}. \end{aligned} \quad (64)$$

Hence, moving rectangular lattice cannot exist at currents $i < i_{\text{min}}$ due to super-radiation as power fed into the crystal should support radiation as well as quasi-particle dissipation needed to ensure stability of this dynamic state. This condition is necessary but it may be not sufficient for the stability of moving rectangular lattice. The ratio of radiation power to that of dissipation one is $r = (\tilde{\omega}_{\text{min}}/\tilde{\omega})^2$. Thus, maximum value of Q is 0.5 at $i = i_{\text{min}}$, and Q drops as current increases beyond i_{min} .

For BSCCO crystals at $\tilde{l} = \pi$ and $b = 1$ we estimate $\tilde{\omega}_{\text{min}} \approx 4$, while $i_{\text{min}} \approx 4 \times 10^{-3}$. At the frequency $\nu = 1$ THz we obtain $\mathcal{P}_{\text{rad}}/w \sim N(\mu\text{W}/\text{cm})$ for $\text{Ti}_2\text{Ba}_2\text{CaCu}_2\text{O}_8$ crystals. Using the energy conservation law, $IV = \mathcal{P}_{\text{rad}}$, we see that to reach this power the total dc current I via the junction should be about 0.004 of the critical current. The radiation power in BSCCO crystals at the same frequency is about 25 times weaker due to smaller Josephson plasma frequency.

Consider now practically more interesting case of moderate number of layers, $\ell < N \ll (k_\omega s)^{-1}$. In this case, from Eq. (60) we obtain the following boundary condition

$$\frac{\partial \theta_\omega(0)}{\partial u} = \frac{i\tilde{\omega}\beta_N}{\ell} \theta_\omega(0), \quad (65)$$

$$\beta_N = \frac{sN}{2\sqrt{\epsilon_c}} \left[|k_\omega| - i \frac{2k_\omega}{\pi} \ln \frac{1}{|k_\omega|sN} \right]. \quad (66)$$

This condition is very similar to the boundary condition (22) for a single junction.

Solving for a_1 and a_2 , we obtain for the edge phase

$$\theta_\omega(0) \approx \frac{\cos(\tilde{\omega}\tilde{l}/\ell) - \exp(-i\tilde{l})}{\ell b \tilde{\omega} [\sin(\tilde{\omega}\tilde{l}/\ell) + i(2\beta_N + v_c \tilde{l}/2\ell) \cos(\tilde{\omega}\tilde{l}/\ell)]} \quad (67)$$

Due to $\beta_N \ll 1$ at small dissipation we obtain the resonant-type I - V characteristics with Fiske

resonances at $\tilde{\omega}\tilde{\ell}/\ell = \pi n$, as in a single JJ. Moreover, for parameters of BSCCO the c -axis quasi-particle dissipation is negligible in comparison with the radiation damping. At resonances we derive

$$i_J = v_c \tilde{\omega} + \frac{1 - (-1)^n \cos(b\tilde{\ell})}{2\tilde{\omega}\ell b^2 \text{Re}[\beta_N]}, \quad (68)$$

The linear approximation brakes down at $2\ell b\tilde{\omega}\text{Re}\beta_N \sim 1$, i.e., it is valid for number of layers $N > \sqrt{\epsilon_c}/(b^2\tilde{\omega}\lambda_{ab}|k_\omega|)$. At the frequency 1 THz linear approximation is valid if $N > 100$. The total radiation power per unit width at the resonance frequency *does not depend on number of layers* and is given by

$$\frac{\mathcal{P}_{\text{rad}}}{w} = \frac{\epsilon_c \Phi_0^2 \omega_p^2}{32\pi^3 \lambda_{ab}^2 \omega b^2} [1 - (-1)^n \cos(b\tilde{\ell})] \quad (69)$$

The independence of this result on N appears as a result of cancellation of the N^2 factor in the total power of N coherently radiating junctions and the factor $\beta_N^{-2} \propto N^{-2}$ which determines the resonance damping. Away from resonances and for resonances limited by quasiparticle damping $\mathcal{P}_{\text{rad}} \propto N^2$. For BSCCO crystals at $\omega/2\pi = 1$ THz, we obtain $\mathcal{P}_{\text{rad}}/w \approx 24$ mW/cm, while for $\text{Tl}_2\text{Ba}_2\text{CaCu}_2\text{O}_8$ crystals we estimate $\mathcal{P}_{\text{rad}}/w \approx 0.5$ W/cm. Now $\tilde{\omega}_{\text{min}}$ and i_{min} become larger as N drops:

$$\tilde{\omega}_{\text{min}}^{3/2} = \left(\frac{\sqrt{\epsilon_c}}{b^2 \tilde{\ell} v_v} \right)^{1/2} \frac{2|\sin(b\tilde{\ell}/2)|}{\sqrt{\omega_p s N/c}}, \quad (70)$$

$$i_{\text{min}} = \frac{3}{2} v_c \omega_{\text{min}}.$$

As N increases beyond $N \sim \ell$. the total radiation power does not depend on N in Fiske resonances and increases $\propto N^2$ outside resonances, while $\tilde{\omega}_{\text{min}}$ decrease as $N^{-1/3}$. This behavior holds until N reaches $(k_\omega s)^{-1}$. After that \mathcal{P}_{rad} increases linearly with N , while $\tilde{\omega}_{\text{min}}$ remains constant.

It is interesting to compare our estimate with recent large-scale simulations of THz radiation out of BSCCO mesa by Tachiki *et al.* [27]. They solve the Maxwell equations coupled with the equations for the intralayer phases inside the crystal and the dielectric media. They found that close to one of the Fiske resonances lattice is mostly disordered but with pronounced rectangular correlations promoted by generated standing electromagnetic wave. They found quite powerful outside radiation in this state, with power density up to $P_x = 3000$ W/cm². Our estimate following from Eq. (69) for 100 junctions occurs to be only slightly smaller ~ 1500 W/cm².

4.5. Triangular Lattice

Triangular lattice, again in the limit $b \gg 1$, behaves quite differently in comparison with rectangular one. The solution has the form

$$\varphi_n(\tau, u) = \tilde{\omega}\tau - bu + \pi n + (-1)^n \phi(\tau, u) + \theta(\tau, u). \quad (71)$$

Here ϕ describes the amplitude of the phase oscillations with Josephson frequency ω , while θ describes oscillations with the frequency 2ω which are induced by moving vortex lattice due to nonlinearity of coupled sine-Gordon equations (46), see [26]. According to theoretical estimates [40] when the lattice velocity approaches the Swihart velocity, the lattice may generate a very powerful electromagnetic wave *inside superconductor*, with power density up to 20 W/cm². Unfortunately, this main harmonic of electromagnetic wave at the frequency ω experiences full internal reflection at the boundary and does not radiate outside. The triangular lattice produce only weak outside radiation at frequency 2ω , caused by the homogeneous in c -direction component of the phase, $\theta(\tau, u)$. In the case of semiinfinite superconductor the radiation power at 2ω has been estimated in by Artemenko and Remizov [26]. Here we estimate this power for finite-size samples when pronounced Fiske resonances are present.

Putting the solution Eq. (71) into Eq. (46), we obtain coupled equations for $\phi(\tau, u)$ and $\theta(\tau, u)$:

$$\frac{\partial^2 \phi}{\partial \tau^2} + \frac{\partial}{\partial \tau} \left(v_c - \frac{v_{ab}}{4} \frac{\partial^2}{\partial u^2} \right) \phi + \frac{1}{4} \frac{\partial^2 \phi}{\partial u^2} = -\sin(\tilde{\omega}\tau - bu), \quad (72)$$

$$\frac{\partial^2 \theta}{\partial \tau^2} + v_c \frac{\partial \theta}{\partial \tau} - \ell^2 \frac{\partial^2 \theta}{\partial u^2} = -\phi \cos(\tilde{\omega}\tau - bu), \quad (73)$$

From the second equation, we see that θ is of order ℓ^{-1} and, as a consequence, terms linear in θ were omitted in the first equation in comparison with the term describing dissipation.

The boundary conditions for the alternating and homogeneous phase are given by

$$\frac{\partial \phi(0)}{\partial u} = 0, \quad \frac{\partial \theta(0)}{\partial u} \approx \pm i\beta\tilde{\omega}\theta(0). \quad (74)$$

for $u = 0, \tilde{\ell}$ with $\beta = 1/\sqrt{\epsilon_c}$. In the framework of the perturbation theory, at $\tilde{\omega}b\alpha_{\text{tr}}\tilde{\ell} \gtrsim 1$, the amplitude ϕ ,

Radiation From Flux Flow in Josephson Junction Structures

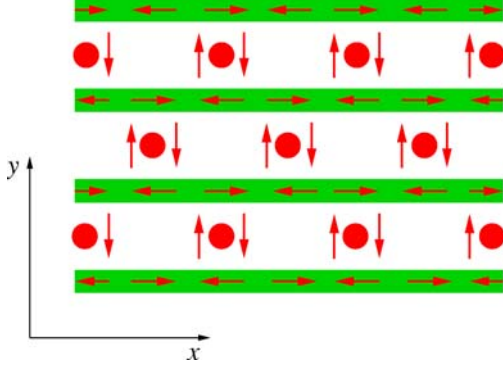


Fig. 9. Triangular lattice of Josephson vortices in layered superconductors. Screening currents compensate each other inside the lattice vortex cell $(2s, 1/b)$ leading to significant reduction of the magnetic energy and enhancement of the amplitude of the phase variations in comparison with rectangular lattice. The in-plane screening currents lead to intralayer quasiparticles contribution to the dissipation of the moving lattice. Due to nonlinearity there are field components at the frequency 2ω with small amplitude. They cause super-radiation at the frequency 2ω .

in the lowest order in $1/b$, is given by the expression

$$\phi = \frac{4[\cos(q(u+l)) - \exp(-ibl) \cos(qu)]}{bq \sin(ql)},$$

$$q = 2\tilde{\omega} + \alpha_{tr}, \quad (75)$$

where $\alpha_{tr} = v_c + v_{ab}\tilde{\omega}^2/4$. Putting it into the equation for θ and accounting for boundary conditions we obtain

$$\theta \approx \frac{i}{2\tilde{\omega}\beta\ell b^3} [1 - \exp(-2ib\tilde{l})] - \frac{[\cos(2\tilde{\omega}\tilde{l}) - \exp(-ib\tilde{l})][1 - \exp(-ib\tilde{l})]}{\omega^2\beta\ell b^2[\sin(2\tilde{\omega}\tilde{l}) + i\alpha_{tr}\tilde{l} \cos(2\tilde{\omega}\tilde{l})]}. \quad (76)$$

Keeping only the resonance term, we obtain the radiation power at the frequency 2ω in the linear regime

$$\mathcal{P}_{rad}(2\omega) \approx \frac{\varepsilon_c \Phi_0^2 \omega_p^4}{2\pi^3 c s^2 \ell^2 \omega^2 b^4} \frac{N}{k_\omega s} \times \frac{[\cos^2(2\tilde{\omega}\tilde{l}) - 2\cos(2\tilde{\omega}\tilde{l})\cos(b\tilde{l}+1)][1 - \cos(b\tilde{l})]}{\sin^2(2(2\tilde{\omega}\tilde{l}) + (\alpha_{tr}\tilde{l})^2 \cos^2(2\tilde{\omega}\tilde{l}))}. \quad (77)$$

Here, as for rectangular lattice, we have large factor $(k_\omega s)^{-1}$ due to super-radiation at the frequency 2ω . This differs from the radiation power for rectangular lattice at the same frequency by the factor of order unity at $\tilde{\omega} \sim 1$ and $b \sim 1$ in the linear regime. Thus,

both rectangular and triangular lattice give approximately the same radiation power for $\tilde{\omega} \sim 1$ and in both cases the radiation is coherent. However, their I - V characteristics and the conversion coefficients Q are very different. The fraction of the power converted into radiation depends on quasiparticle conductivities σ_{ab} and σ_c . These conductivities remain nonzero in cuprate superconductors even if temperature approaches zero because cuprates are gapless superconductors. As a result, only small part, of order $(b^2 \ell^2 \alpha_{tr} \tilde{l})^{-1}$, is converted into the radiation in the linear regime. Thus, for triangular lattice we estimate very small $Q \propto \ell^{-2}$. This translates into strong heating and practically triangular lattice cannot provide a realistic source of radiation.

The I - V characteristics is determined by the behavior ϕ and so it is resonant at low dissipation, as in a single JJ. In particular, for (i) weak dissipation, $q \approx 2\tilde{\omega} + i\alpha_{tr}$, and (ii) small frequencies $\tilde{\omega} \ll b/2$ we obtain

$$i_J \approx \frac{8}{b^4} \alpha_b \tilde{\omega} + \frac{2\alpha_b [\cos(2\tilde{\omega}\tilde{l}) - \cos(b\tilde{l})] \cos(2\tilde{\omega}\tilde{l})}{\tilde{\omega} b^2 [\sin^2(2\tilde{\omega}\tilde{l}) + (\alpha_{tr} \tilde{l})^2 \cos^2(2\tilde{\omega}\tilde{l})]}, \quad (78)$$

where $\alpha_b = v_c + v_{ab}b^2$ and $\alpha_{tr} = v_c + v_{ab}\tilde{\omega}^2$. The amplitude of the Fiske peak at $2\tilde{\omega}_n \tilde{l} = \pi n$ is

$$\delta_n i_J \approx \frac{2[1 - (-1)^n \cos(b\tilde{l})]}{\tilde{\omega}_n b^2 \tilde{l}^3 (v_c + v_{ab}\tilde{\omega}_n^2)}. \quad (79)$$

Note that triangular lattice excites resonances for the antiphase modes whose frequencies are by factor $2\ell = 2\lambda ab/s \sim 300$ smaller than the frequencies of the homogeneous modes excited by the rectangular lattice. Very pronounced Fiske steps have been observed recently by Kim *et al.* [23]

We also estimated that the lattice with random parameters κ_n gives incoherent radiation with approximately the same power and the conversion coefficient as triangular lattice.

5. CONCLUSIONS

We have estimated the radiation power from most probable vortex lattices in the large- N limit. Our estimate for rectangular lattice in BSCCO agrees satisfactory with results of numerical study by Tachiki *et al.* [27]. We see that only rectangular lattice gives significant radiation power and quite high conversion coefficient, i.e., up to half power fed into the crystal may be converted into the radiation. Thus, not very high currents are needed

to get significant radiation power. However, the main question to be answered is what are parameters of the stability of rectangular lattice in finite-size samples. Other open questions include the following:

1. What is the radiation power in highly nonlinear regime for triangular lattice and for rectangular lattice with moderate number of layers N ?
2. What is the structure of steady states and the radiation power of crystals with not very large $N < \ell$, when the boundaries along the y -axis become important?
3. What are boundary conditions and the radiation power in crystals with $wk_\omega \ll 1$?
4. Are there *fully gapped* layered superconducting materials or artificial multilayer system which can be used as radiation sources? Presence of finite gap in the whole Fermi surface drastically reduces quasiparticle dissipation at low temperatures and the problem of high dissipation for the moving triangular lattice in the high-temperature superconductors will be avoided.
5. Is it possible to get stronger radiation from the triangular lattice by modulating the radiated end phase of the crystal? For example, one can use some periodic layer of dielectric or metal between the crystal and the air which may result in more effective conversion of high k_y electromagnetic fields inside the crystal into low k_y outside electromagnetic waves. For that the surface modulation has to have the periodicity $2s$, i.e., every second layer has to be closed. For efficient conversion, one can anticipate that the radiation power would be larger by the factor $\ell^2 \approx 10^4$ in BSCCO and TBCCO crystals.

ACKNOWLEDGMENTS

The authors thank Yu. Galperin, A. Gurevich, I. Martin, K. Rasmussen, N. Grønbech-Jensen, and R. Kleiner for useful discussions. This research was supported by the Department of Energy under contracts #W-7405-ENG-36 (LANL) and # W-31-109-ENG-38 (Argonne).

REFERENCES

1. B. D. Josephson, *Phys. Lett.* **1**, 251 (1962).
2. I. M. Dmitrenko, I. K. Yanson, and V. M. Svistunov, *Pis'ma ZhETF* **2**, 134 (1965); I. K. Yanson, *Low Temp. Phys.* **30**, 516 (2004).
3. D. N. Langenberg, D. J. Scalapino, B. N. Taylor, and R. E. Rice, *Phys. Rev. Lett.* **15**, 294 (1965).
4. J. Swihart, *J. Appl. Phys.* **32**, 461 (1961).
5. I. O. Kulik and I. K. Yanson, *The Josephson Effect in Superconducting Tunneling Structures*, Jerusalem, 1972.
6. A. V. Ustinov, *Physica D* **123**, 315 (1998).
7. N. F. Pedersen and A. V. Ustinov, *Superc. Sci. Technol.* **8**, 389 (1995).
8. A. K. Jain, K. K. Likharev, J. E. Lukens, and J. E. Sauvageau, *Phys. Rep.* **109**, 309 (1984).
9. R. Kleiner, *Phys. Rev. B* **50**, 6919 (1994).
10. Ustinov and S. Sakai, *Appl. Phys. Lett.* **73**, 686 (1998).
11. Yu. M. Ivanchenko, *Phys. Rev. B* **54**, 13247 (1996).
12. M. Darula, T. Doderer, and S. Beuven, *Supercond. Sci. Technol.* **12**, R1 (1999).
13. W. E. Lawrence and S. Doniach, in *Proceedings of the 12th International Conference on Low Temperature Physics, Kyoto 1970*, E. Kanda, ed. (Keigaku, Tokyo, 1970).
14. R. Kleiner, F. Steinmeyer, and P. Müller, *Phys. Rev. Lett.* **68**, 2394 (1992); R. Kleiner and P. Müller, *Phys. Rev. B* **49**, 1327 (1994).
15. Yu. I. Latyshev, J. E. Nevelskaya, and P. Monceau, *Phizika Nizkikh Temperatur* **22**, 629 (1996).
16. M. B. Gaifullin, Y. Matsuda, and L. N. Bulaevskii, *Phys. Rev. Lett.* **81**, 3551 (1998).
17. O. K. C. Tsui, N. P. Ong, Y. Matsuda, Y. F. Yan, and J. B. Peterson, *Phys. Rev. Lett.* **73**, 724 (1994); O. K. C. Tsui, N. P. Ong, and J. B. Peterson, *Phys. Rev. Lett.* **76**, 819 (1996).
18. Y. Matsuda, M. B. Gaifullin, K. Kumagai, K. Kadowaki, and T. Mochiku, *Phys. Rev. Lett.* **75**, 4512 (1995); Y. Matsuda, M. B. Gaifullin, K. Kumagai, K. Kadowaki, and K. Hirata, *Phys. Rev. Lett.* **78**, 1972 (1997); Y. Matsuda, M. B. Gaifullin, K. Kumagai, K. Kadowaki, Mochiku, and K. Hirata, *Phys. Rev. Lett.* **75**, 4512 (1995).
19. H. B. Wang, P. H. Wu, and T. Yamashita, *Phys. Rev. Lett.* **87**, 107002 (2001).
20. Yu. I. Latyshev, M. B. Gaifullin, T. Yamashita, M. Machida, and Y. Matsuda, *Phys. Rev. Lett.* **87**, 247007 (2001).
21. A. Irie, Y. Hirai, and G. Oya, *Appl. Phys. Lett.* **72**, 2159 (1998).
22. V. M. Krasnov, N. Mros, A. Yurgens, and D. Winkler, *Phys. Rev. B* **59**, 8463 (1999).
23. S.-M. Kim, H. B. Wang, T. Hatano, S. Urayama, S. Kawakami, M. Nagao, T. Takano, T. Yamashita, and K. Lee, *Phys. Rev. B* **72**, R140504 (2005).
24. T. Koyama and M. Tachiki, *Sol. St. Comm.* **96**, 367 (1995).
25. Yu. I. Latyshev, M. B. Gaifullin, T. Yamashita, M. Machida, and Y. Matsuda, *Phys. Rev. Lett.* **87**, 247007 (2001).
26. S. N. Artemenko and S. V. Remizov, *Physica C* **362**, 200 (2000).
27. M. Tachiki, M. Iizuka, S. Tejjima, and H. Nakamura, *Phys. Rev. B* **71**, 134515 (2005).
28. G. Hechtfisher, R. Kleiner, A. V. Ustinov, and P. Müller, *Phys. Rev. Lett.* **79**, 1365 (1997).
29. K. Kadowaki, *Joint JSPS and ESF Conference on Vortex Matter in Nanostructured Superconductors (VORTEX IV)*, 3–9 September 2005, Crete, Greece.
30. I. E. Batov, X. Y. Jin, S. V. Shitov, V. Koval, P. Muller, and A.V. Ustinov, preprint.
31. I. O. Kulik, *Pis'maZhETF* **2**, 134 (1965) [*JETP Lett.* **2**, 84 (1965)].
32. M. Cirillo, N. Grønbech-Jensen, M. R. Samuelsen, M. Salerno, and G. V. Rinati, *Phys. Rev. B* **58**, 12377 (1998).

Radiation From Flux Flow in Josephson Junction Structures

33. J.-J. Chang, *Phys. Rev. B* **28**, 1276 (1983).
34. R. Simmonds, K. M. Lang, D. A. Hite, D. P. Pappas, and J. M. Martinis, *Phys. Rev. Lett.* **93**, 035301 (2004).
35. A. Gurevich, *Phys. Rev. B* **46**, 3187 (1992).
36. L. N. Bulaevskii, M. Zamora, D. Baeriswyl, H. Beck, and J. R. Clem, *Phys. Rev. B* **50**, 12831 (1994).
37. R. Kleiner, P. Müller, H. Kohlstedt, N. F. Pedersen, and S. Sakai, *Phys. Rev. B* **50**, 3942 (1994).
38. L. N. Bulaevskii, D. Dominguez, M. P. Maley, A. R. Bishop, and B. I. Ivlev, *Phys. Rev. B* **53**, 14601 (1996).
39. A. E. Koshelev and L. N. Bulaevskii, *Phys. Rev. B* **62**, 14403 (2000).
40. A. E. Koshelev and I. Aranson, *Phys. Rev. Lett.* **85**, 3938 (2000); *Phys. Rev. B* **64**, 174508 (2001).
41. S. N. Artemenko and S. V. Remizov, *Phys. Rev. B* **67**, 144516 (2003).
42. A. E. Koshelev, *Physica C* **435** (2006).
43. S. Ooi, T. Mochiku, and K. Hirata, *Phys. Rev. Lett.* **89**, 247002 (2002).
44. Yu. I. Latyshev, A. E. Koshelev, and Bulaevskii, *Phys. Rev. B* **68**, 134504 (2003).
45. V. K. Thorsmølle, R. D. Averitt, M. P. Malcy, L. N. Bulaevskii, C. Helm, and A. J. Taylor, *Opt. Lett.* **26**, 1292 (2001).